Hiding the interior region of core-shell nanoparticles with quantum invisible cloaks

Jeng Yi Lee[1,*] and Ray-Kuang Lee[1,2]
[1]*Institute of Photonics Technologies, National Tsing-Hua University, Hsinchu 300, Taiwan*
[2]*Physics Division, National Center of Theoretical Science, Hsinchu 300, Taiwan*
(Received 10 June 2013; revised manuscript received 9 April 2014; published 22 April 2014)

Based on the scattering cancellation, we provide a method not only making a nanoparticle nearly invisible, but also hiding its interior region from the outside probing matter wave. By applying the interplay among the nodal points of partial waves along with the concept of streamline in fluid dynamics for probability flux, a quantum invisible cloak to the electron transport in a host semiconductor is demonstrated by simultaneously guiding the probability flux outside a hidden region and keeping the total scattering cross section negligible. As the probability flux vanishes in the interior region, one can embed any materials inside a multiple core-shell nanoparticle without affecting physical observables from the outside. Our results reveal the possibility to design a protection shield layer for fragile interior parts from the impact of transport electrons.

DOI: 10.1103/PhysRevB.89.155425 PACS number(s): 78.67.Pt, 03.75.−b, 72.20.Dp, 73.63.−b

I. INTRODUCTION

A transformation method, originally proposed to control electromagnetic (EM) waves [1,2], has been applied to a broad area of physical systems from acoustics [3], quantum matter waves [4–7], fluid dynamics [8], and thermodynamics [9]. By avoiding any scattering and preventing waves from entering the interior region, *invisible cloaking* devices operating at a specific frequency were realized experimentally for EM waves with the fabrication of metamaterials [10]. However, for matter waves, the application of a transformation method to a spherical quantum object requires the corresponding effective mass and potential being radially dependent in geometry, resulting in an infinite value in the inner cloaking layer [4].

Instead of using functionally graded metamaterials, another way to have a nearly invisible cloaking is achieved by the scattering cancellation method, through the elimination of major contributed scattered waves for the structures at the subwavelength scale. Alú and Engheta demonstrated that in the EM case, an object coated by isotropic and homogeneous metamaterials or plasmonics can generate a pair of positive-negative polarizations to diminish the electric dipole moment [11,12]. Due to the similar mathematical structure between the time-independent Schrödinger equation and Helmholtz wave equation, a barrier-well potential formed in a core-shell nanoparticle embedded in a host semiconductor is found to become almost invisible for the transport electron matter wave [13]. By simultaneously eliminating the scattered s (monopole) and p (dipole) waves, a quantum cloak may be realized in state-of-the-art solid state systems, such as quantum dots, graphene, and thermoelectrics [14–16]. Furthermore, the scattering cancellation method is a nonresonant mechanism [17], making it possible to allow some tunable range for the cloaking conditions.

Even though the core-shell nanoparticle is invisible from not being detected by the conduction electrons with a typical energy scale in semiconductors, the probability flux of the matter wave still passes through the entire nanoparticle. In this scenario, unless the required cloaking parameters of a delicate functional device matches well, a slight change of physical parameters in the core region may result in a severe degradation of the scattering cross section [18]. As transformation optics demonstrates, an *invisible cloak* should prevent fields from entering the region, as well as avoid any scattering in the region around simultaneously. In order to hide from the incident matter wave, to be invisible and cloaking at the same time, in this paper we demonstrate the possibility to make a nanosphere invisible as well as to guide the probability flux outside the interior region, by applying the conservation of probability flux as the streamline in fluid dynamics. To guide the probability flux of quantum matter waves outside the hidden region, a destructive interference between the incoming and outgoing spherical traveling waves in the shell region is required, resulting in the total internal reflection at the core-shell interface. With our systematic approach to guide the probability flux outside the core-region, even a simple core-shell nontransparent object can be hidden from the probing matter waves. With the introduction of above two degrees of freedom, our method differs from the generalization of known results on quantum invisible cloaks. Moreover, by considering nanoparticles in the shape of a multiple core-shell sphere, we reveal a quantum invisible cloak to the electron transport in a host semiconductor, in which one can embed any material inside the hidden region without affecting physical observables from the outside. The robustness to hide any material inside a protection region is also demonstrated in a multilayer structure for a wide range of parameters.

II. CONDITIONS FOR BEING INVISIBLE AND HIDDEN SIMULTANEOUSLY

As illustrated in Fig. 1, we begin with a spherical nanoparticle, composed of two concentric layers of isotropic and homogeneous materials (a core-shell structure), with a different effective mass and potential energy defined in each region. Consider an electron with the energy E, an effective mass m_0, and characteristic incident plane matter wave Ψ_i propagating along the z axis. The corresponding wave number outside the nanoparticle is defined as $k_0 = \sqrt{2m_0(E - V_0)}/\hbar$, where the potential energy in the background environment is set to zero, $V_0 = 0$. In the shell region, the effective mass and potential are denoted by m_s and $V_s < 0$, respectively,

*johnnyygod2002@hotmail.com

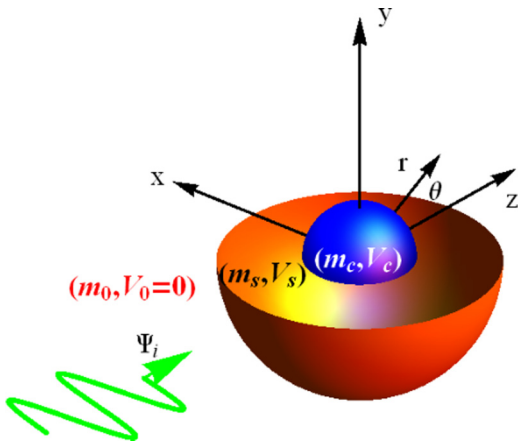

FIG. 1. (Color online) A nanoparticle with the core-shell structure is illustrated as our quantum invisible cloak, where a different effective mass and potential energy are defined in each region, respectively. The quantum matter plane wave for the transport electron Ψ_i is assumed to propagate along the z axis.

with the corresponding wave number $k_s = \sqrt{2m_s(E-V_s)}/\hbar$; while in the core region, the effective mass, potential, and wave number are denoted as m_c, $V_c > 0$, and $k_c = \sqrt{2m_c(E-V_c)}/\hbar$, respectively. Geometrical parameters for the core-shell nanoparticle are the radius of the core, a_c, and the radius of the whole particle, a.

Following the partial wave analysis for a time-independent nonrelativistic Schrödinger equation with an incident plane wave Ψ_i [19], one can decompose the matter wave solution outside the nanoparticle into $\Psi_0(r,\theta) = \Psi_i + \Psi_{\rm scat} = \sum_{l=0}^{l=\infty} i^l(2l+1)\{j_l(k_0r) + a_l^{\rm scat}h_l^{(1)}(k_0r)\}P_l(\cos\theta)$, with the complex coefficient $a_l^{\rm scat}$ for the scattering matter wave $\Psi_{\rm scat}$. By the same way, the corresponding wave solutions in the shell and core regions have the form: $\Psi_s(r,\theta) = \sum_{l=0}^{l=\infty} i^l(2l+1)\{b_l j_l(k_sr) + c_l h_l^{(1)}(k_sr)\}P_l(\cos\theta)$ and $\Psi_c(r,\theta) = \sum_{l=0}^{l=\infty} i^l(2l+1)d_l j_l(k_cr)P_l(\cos\theta)$, respectively. Here, b_l, c_l, and d_l are the characteristic complex coefficients for the infinite series of the partial waves in each region, with j_l, $h_l^{(1)}$, and P_l being the lth-order spherical Bessel function, spherical Hankel function of the first kind, and Legendre function, respectively. By matching the boundary conditions at each boundary to satisfy the continuity of the wave function and the conservation of probability flux in the radial direction r, we can find the corresponding complex coefficients.

Based on the scattering cancellation method [11–13], we assume that there exists a set of parameters to support an invisible and hidden nanoparticle (this assumption should be verified afterward). In this case, we have $a_l^{\rm scat} = 0$ for $l = 0,1$ and $a_l^{\rm scat} \approx 0$ for $l \geqslant 2$ (its absolute value is smaller than 10^{-3}). Then, under above approximation, the corresponding coefficients b_l and c_l for the wave function in the shell region, Ψ_s, can be found in a closed form,

$$b_l^{app} \approx \frac{x_2y_1j_l(x_1)h_l^{(1)'}(x_2) - x_1y_2h_l^{(1)}(x_2)j_l'(x_1)}{x_2y_1j_l(x_2)h_l^{(1)'}(x_2) - x_2y_1h_l^{(1)}(x_2)j_l'(x_2)}, \quad (1)$$

$$c_l^{app} \approx \frac{x_1y_2j_l(x_2)j_l'(x_1) - x_2y_1j_l(x_1)j_l'(x_2)}{x_2y_1j_l(x_2)h_l^{(1)'}(x_2) - x_2y_1h_l^{(1)}(x_2)j_l'(x_2)}, \quad (2)$$

where the shorthanded notations used are $j_l'(x) \equiv dj_l(x)/dx$, $h_l^{(1)'}(x) \equiv dh_l^{(1)}(x)/dx$, $x_1 \equiv k_0a$, $y_1 \equiv m_0a$, $x_2 \equiv k_sa$, and $y_2 \equiv m_sa$. By transforming the shell wave function bases into the pair of Hankel functions of the first and the second kinds, $h_l^{(1)}$ and $h_l^{(2)}$, the corresponding coefficients for the outgoing and incoming waves are $i^l(2l+1)(b_l^{app}/2 + c_l^{app})$ and $i^l(2l+1)b_l^{app}/2$, respectively [19]. Moreover, the condition $|b_l^{app}/2 + c_l^{app}| = |b_l^{app}/2|$ is valid for any real parameters, which means that each partial wave forms a kind of standing wave in the shell region. With the above physical insights, we look for a total internal reflection at the core-shell interface, by imposing a destructive interference between the outgoing and incoming spherical traveling waves. As the Goos-Hänchen phase shift happens in the total internal reflection [20], here, we look for the wave solution Ψ_s with a nodal point occurring at the neighboring interface of the core-shell, in order to form a hidden region. In other words, instead of finding the separating nodal point for each partial wave inside the shell region, to hide a nontransparent object our first condition to be satisfied is to set the nodal points of Ψ_s penetrating a little into the core region. Even though, the position of this nodal point within the core region should be related to the effective mass and potential, in the following we set this nodal point as an additional degree of freedom, which is not specified.

In addition, by the conservation of probability flux, one has $\vec{\nabla}\cdot\vec{J}_k = 0$, where $\vec{J}_k = (e\hbar/m_k)\,{\rm Im}[\Psi_k^*\nabla\Psi_k]$, with m_k and Ψ_k corresponding to the effective mass and wave function in each region ($k = 0,s,c$ for the outside, shell, and core regions, respectively) [21]. To have an invisible cloak to support a hidden region, we assume that almost all of the probability flux flows in the shell region, that is,

$$\int_0^{2\pi}\int_{a_c}^{a}\hat{z}\cdot\vec{J}_s\left(r,\theta=\frac{1}{2}\pi\right)rdrd\phi = \pi a^2\frac{e\hbar k_0}{m_0}(1-\epsilon), \quad (3)$$

where $\vec{J}_s$ is approximately orthogonal to the x-y plane at the polar angle $\theta = \frac{\pi}{2}$. Here, an infinitesimal parameter ϵ is introduced to measure the loss of total flux due to any possible quantum tunneling effect that occurred at the potential interfaces. In general, if ϵ is chosen too small, a higher barrier potential for the core and a lower potential well for the shell is required. Our numerical results reveal that the value of ϵ can be chosen with an arbitrarily small value, but to have a practical parameter set, in the following, we set $\epsilon = 0.06$ as an illustration. Basically, as is the case in fluid dynamics, Eq. (3) enforces the streamline of the probability flux to flow in the shell region.

For a given geometrical structure, the size parameters a and a_c are given. Then, with the introduction of these two additional conditions: to seek a nodal point for the wave solution Ψ_s penetrating into the core region due to the total internal reflection, and to have a conserved probability flux in the shell region, it is sufficient to determine two physical parameters in the shell region. In Fig. 2(a), we report the parameter set $\{m_s, V_s\}$ to support a quantum invisible cloak numerically for the wave function in the shell region Ψ_s with a nodal point within the core region, $|\Psi_s(r_n)| = 0$ at $r_n < a_c$. The found wave function in the shell region is shown in Fig. 2(c), with the comparison to the decomposed channel

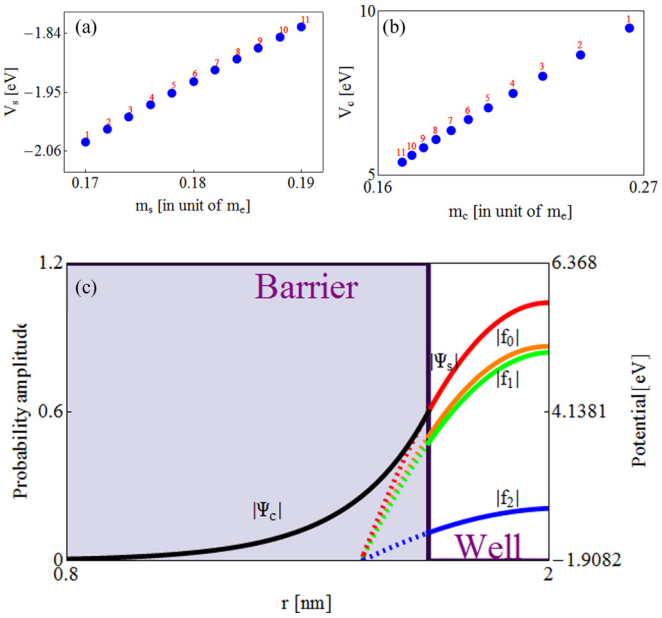

FIG. 2. (Color online) (a) The parameter set $\{m_s, V_s\}$ to support a total internal reflection for the wave function in the shell region, Ψ_s; and (b) the corresponding parameter set $\{m_c, V_c\}$, marked in numbers, to simultaneously generate a negligible total normalized scattering cross section, as small as 10^{-4}. (c) The probability amplitude of wave functions inside the barrier-well potential, as a function of the radial axis r, are shown for $|\Psi_c|$ and $|\Psi_s|$ in black and red colors, respectively. Decomposed channel functions f_l, $l = 0,1,2$, are also shown as a comparison. Moreover, dashed lines in the barrier region show the extension of wave functions from the shell (potential well) region, all of which have a common nodal point. The parameter set $\{m_s, V_s, m_c, V_c\}$ used in (c) is $\{0.182m_e$, -1.91 eV, $0.1901m_e$, 6.368 eV$\}$, with the geometric size parameters of our nanoparticle: $a = 2$ and $a_c = 1.7$ nm. The energy and effective mass for the transport electron are $E = 0.01$ eV and $m_0 = 0.8m_e$ (in unit of the electron mass m_e), respectively.

function defined as $f_l(r,\theta = 0) = i^l(2l+1)\{b_l j_l(k_s r) + c_l h_l^{(1)}(k_s r)\}P_l(\cos\theta)$, for different l. As shown in Fig. 2(c), the contribution from higher-order terms of partial waves are significantly small enough as expected. Moreover, such a nodal point penetrates into the core region because of wave tunneling, as in the case of a Goos-Hänchen phase shift in the total internal reflection. Since we have a spherical symmetry in geometry, the requirement to have a nodal point solution for all the polar angle θ values results in guiding the probability flux to flow in the shell region with a nontrivial solution.

Then, with the set of solutions $\{m_s, V_s\}$ found in Fig. 2(a), we search for the corresponding set of parameters $\{m_c, V_c\}$ by coming back to the concept of scattering cancellation [11–13]. The scattering cross section outside the particle has the form $\sigma = \frac{4\pi}{k_0^2}\sum_{l=0}^{l=\infty}(2l+1)|a_l^{\rm scat}|^2$, with the complex scattering coefficient $a_l^{\rm scat}$ defined as

$$a_l^{\rm scat} = -\frac{x_1 j_l'(x_1)[A_l + B_l] + y_1 j_l(x_1)[C_l + D_l]}{x_1 h_l'(x_1)[A_l + B_l] + y_1 h_l(x_1)[C_l + D_l]}, \quad (4)$$

where

$$A_l = y_2 x_3 y_4 j_l(x_4)[j_l(x_2)h_l'(x_3) - h_l(x_2)j_l'(x_3)], \quad (5)$$

$$B_l = y_2 y_3 x_4 j_l'(x_4)[h_l(x_2)j_l(x_3) - j_l(x_2)h_l(x_3)], \quad (6)$$

$$C_l = x_2 x_3 y_4 j_l(x_4)[h_l'(x_2)j_l'(x_3) - h_l'(x_3)j_l'(x_2)], \quad (7)$$

$$D_l = x_2 y_3 x_4 j_l'(x_4)[j_l'(x_2)h_l(x_3) - h_l'(x_2)j_l(x_3)]. \quad (8)$$

Here, the shorthanded notations used are $x_3 \equiv k_s a_c$, $x_4 \equiv k_c a_c$, $y_3 \equiv m_s a_c$, and $y_4 \equiv m_c a_c$.

Based on Eq. (4), the set of parameters $\{m_c, V_c\}$ found to support an invisible cloak is shown in Fig. 2(b), with the one-to-one corresponding markers to the set of parameters $\{m_s, V_s\}$ shown in Fig. 2(a), which confine the probability flux in the shell region simultaneously. By our proposed method, the parameter set $\{m_s, V_s, m_c, V_c\}$ generates a quantum invisible cloak to hide a nontransparent object, which support almost zero values both for the total scattering cross section and probability flux in the core region simultaneously. As a comparison, in Figs. 3(a) and 3(b), we use the parameters reported in Ref. [13] to demonstrate the known results on a quantum invisible cloak. Even though this nanoparticle is invisible as shown in Fig. 3(a), but the probability flux goes through the entire object as shown in Fig. 3(b). In this scenario, a slight change of physical parameters in the interior region may result in a severe degradation of the scattering cross section [14].

Instead, in Figs. 3(c) and 3(d), we plot the distributions of probability density and probability flux, respectively, for hiding a nontransparent object by our systematical approach. With the parameters shown in Fig. 2(c), it can be seen that almost all the probability flux circulates along the boundary of the barrier-well potential, while inside the core region the probability flux is almost zero. The comparison between Figs. 3(b) and 3(d) clearly demonstrates the difference between our method and others. Take the simulation shown in Figs. 3(c) and 3(d) as an example; the probability to find the matter wave inside the core region is as small as 10^{-5} at $r = 0.5a_c$ and about 10^{-7} at $r = 0$, while the total normalized scattering cross section is kept negligible at 10^{-4}. We want to remark that in the calculations, we do not restrict ourselves by truncating the infinite series for the scattering cross section and the corresponding probability flux. Instead, we calculate as many as possible terms to satisfy the conditions that the value of each term is smaller than 10^{-5}.

III. DISCUSSION ON THE EXISTENCE OF A HIDDEN REGION

Since in our proposed method the nodal point of the wave function is chosen to be located outside the shell region, a little amount of the probability flux still penetrate into the core region, about $\epsilon\pi a^2 e\hbar k_0/m_0$. In this case, for a simple barrier-well potential only, we can not take this core region as an ideal hidden region. To hide the interior perfectly, we extend our method for a nanoparticle in the shape of multiple core-shell spheres. Take a three-layer potential as an example; now, it is possible to construct a hidden interior region for $a_h < a_c$, where a_h is the radius of the interior hidden region. If the thickness of the core region is thin, as expected, a

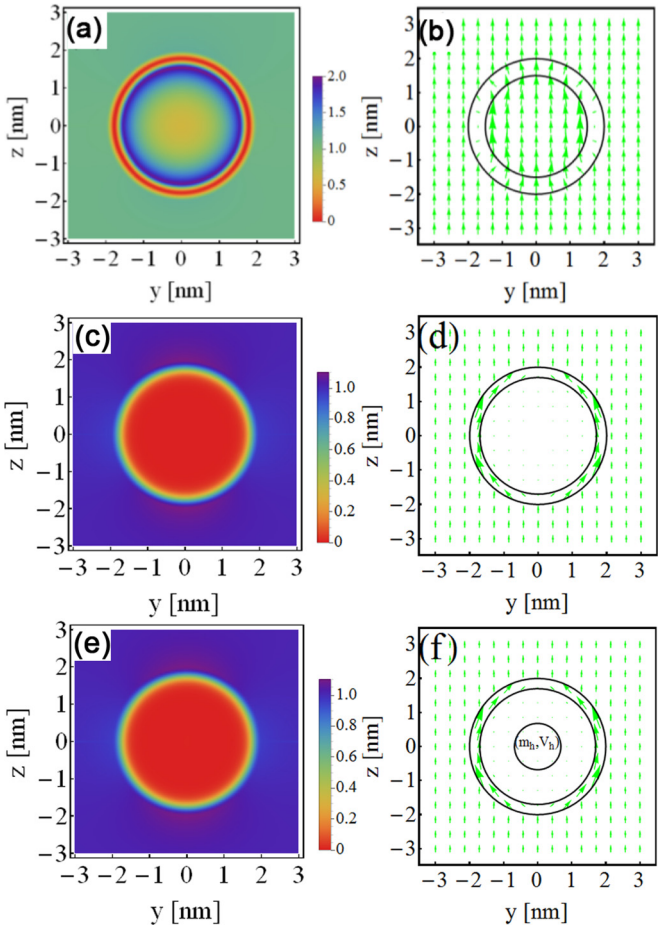

FIG. 3. (Color online) (a) Probability density $|\Psi|^2$, and (b) the corresponding probability flux $\vec{J}$ of the wave function in the plane $x = 0$ for a quantum invisible cloak, with the parameters reported in Ref. [13]. Even though this nanoparticle is invisible as shown in (a), but from (b) it can be seen that the probability flux goes through the entire object. Instead, (c) and (d) show the probability density and the corresponding probability flux, respectively, for hiding a nontransparent object, with the same parameter set used in Fig. 2(c). In this simulation, the probability inside the core region is calculated as small as 10^{-7}, while near the interface of the core-shell, a probability flux is generated to satisfy the conservation of probability flux. Moreover, a three-layer nanoparticle as a quantum invisible cloak is demonstrated in (e) and (f), with the corresponding probability density and flux, respectively. Here, the parameters used are $a = 2$, $a_c = 1.7$, $a_h = 0.68$ nm, $m_0 = 0.8m_e$, $m_s = 0.182m_e$, $m_c = 0.19m_e$, $m_h = 0.5m_e$, $V_s = -1.91$, $V_c = 6.368$, $V_h = -20$, and $E = 0.01$ eV, respectively.

change of any parameter in the hidden region would modify the scattering properties in the outside. Instead, if the thickness is thick enough to exclude the quantum tunneling effect, then the total scattering cross section remains nearly unchanged no matter what kind of material is placed inside the interior region, as shown in Figs. 3(e) and 3(f). Moreover, within such a hidden region, we test a wide range of parameters for the object embedded inside. For the effective mass as large as $10m_e$ ($m_h = [0, 10m_e]$) and the effective potential in the hidden region from -30 to $+30$ eV, the corresponding scattering cross section remains unchanged. This result implies that our hidden region in a three-layer structure is indeed strongly robust even with such an extreme set of parameters.

Before our conclusion, we want to remark that a one-dimensional (1D) configuration is known for not being able to provide the transmission resonance (invisible) and shield (cloaking) simultaneously. In our approach, a potential well is chosen to create a region with a high probability flux, in order to compensate for the forbidden flow in the hidden region. Our results may remind people that the generalization of concepts about the bound states in the antiresonance from 1D to higher dimensions should be revisited. This is very important for the future study on the scattering in nanoscales. Moreover, in the typical scattering cancellation method, the values of $k_s a$ and $k_c a_c$ are small enough in each layer to approximate the quasistatic limit. This limit is equivalent to the solution of Laplace equation in the electrostatics potential [22]. We want to remark that, in our case, to support a negligible scattering cross section, we follow the guideline that $k_0 a < 1$ outside the nanoparticle, but have $|k_s a| = 6.06$ and $|k_c a| = 11.27$, in the shell and core regions, respectively, both of which are greater than 1.

IV. CONCLUSIONS

In conclusion, we introduce two more degrees of freedom to construct a quantum invisible cloak, by requiring the total internal reflection and the conservation of probability flux in the shell region. Solutions of wave function in the shell region are required to have a nodal point penetrating into the core region, resulting in guiding the probability flux only circulating in the shell region. With our approach, one can embed any material inside the hidden region without disturbing the probing matter wave from the outside. Our results provide a systematical way to hide nontransparent objects at the subwavelength scale. In this scenario, we do not need to worry about the design for cloaking different objects. Moreover, this hidden region can also provide a protective shield for some sensitive or easily corrupted devices from the impact of transport electrons. With the analogy between quantum matter waves and classical waves, the concept of our method can be readily applied in other fields, such as electromagnetic and acoustic systems, etc.

[1] U. Leonhardt, Science **312**, 1777 (2006).
[2] J. B. Pendry, D. Schurig, and D. R. Smith, Science **312**, 1780 (2006).
[3] S. A. Cummer, B.-I. Popa, D. Schurig, D. R. Smith, J. Pendry, M. Rahm, and A. Starr, Phys. Rev. Lett. **100**, 024301 (2008).
[4] S. Zhang, D. A. Genov, C. Sun, and X. Zhang, Phys. Rev. Lett. **100**, 123002 (2008).
[5] D. H. Lin, Phys. Rev. A **81**, 063640 (2010).
[6] D. H. Lin, Phys. Rev. A **85**, 053605 (2012).
[7] A. Greenleaf, Y. Kurylev, M. Lassas, and G. Uhlmann, Phys. Rev. Lett. **101**, 220404 (2008).

[8] Y. A. Urzhumov and D. R. Smith, Phys. Rev. Lett. **107**, 074501 (2011).
[9] S. Guenneau, C. Amra, and D. Veynante, Opt. Express **20**, 8207 (2012).
[10] D. Schurig, J. J. Mock, B. J. Justice, S. A. Cummer, J. B. Pendry, A. F. Starr, and D. R. Smith, Science **314**, 977 (2006).
[11] A. Alu and N. Engheta, Phys. Rev. E **72**, 016623 (2005).
[12] A. Alu and N. Engheta, Opt. Express **15**, 3318 (2007).
[13] B. L. Liao, M. Zebarjadi, K. Esfarjani, and G. Chen, Phys. Rev. Lett. **109**, 126806 (2012).
[14] R. Fleury and A. Alu, Phys. Rev. B **87**, 045423 (2013).
[15] B. L. Liao, M. Zebarjadi, K. Esfarjani, and G. Chen, Phys. Rev. B **88**, 155432 (2013).
[16] M. Zebarjadi, B. L. Liao, K. Esfarjani, M. S. Dresselhaus, and G. Chen, Adv. Mater. **25**, 1577 (2013).
[17] A. Alu and N. Engheta, J. Opt. A-Pure Appl. Op. **10**, 093002 (2008).
[18] C. F. Bohren and D. R. Huffman, *Absorption and Scattering of Light by Small Particles* (Wiley, New York, 1983).
[19] G. J. Gbur, *Mathematical Methods for Optical Physics and Engineering* (Cambridge University Press, Cambridge, 2011).
[20] H. A. Haus, *Waves and Fields in Optoelectronics* (Prentice-Hall, Inc., Englewood Cliffs, NJ, 1984).
[21] A. F. J. Levi, *Applied Quantum Mechanics*, 2nd ed. (Cambridge University Press, Cambridge, 2006).
[22] D. J. Griffiths, *Introduction to Electrodynamics*, 3rd ed. (Prentice Hall, Inc., Upper Saddle River, New Jersey, 1999).